Science Letters ISSN 2345-5463 DOI: https://doi.org/10.47262/SL/9.2.132021007

Research article
2021 | Volume 9 | Issue 2 | Pages 42-48

ARTICLE INFO

Received
March 05, 2021
Revised
May 21, 2021
Accepted
May 23, 2021
Published
June 26, 2021

***Corresponding author**
Damilohun Samuel Metibemu
E-mail
damilohun.metibemu@aaua.edu.ng
Phone
+2348072640512

Keywords
Cancer
Cyclin-dependent kinase 4
Molecular docking
Phytochemicals
3D-QSAR

How to cite
Metibemu DS. 3D-QSAR and molecular docking approaches for the identification of novel phyto-inhibitors of the cyclin-dependent kinase 4. Sci Lett 2021; 9(2):42-48

Open Access

3D-QSAR and Molecular Docking Approaches for the Identification of Novel Phyto-inhibitors of the Cyclin-dependent Kinase 4

Damilohun Samuel Metibemu*

Department of Biochemistry, Adekunle Ajasin University, Akungba-Akoko, Ondo State, Nigeria

Abstract

Cyclin-dependent kinase 4 (CDK4) is an important target in designing anti-cancer drugs. The activation of CDK4 results in phosphorylation of the retinoblastoma gene product. In this study, a total of one hundred and seventy-eight phytochemicals characterized from various anti-cancer plants were retrieved from the literature and screened against the orthosteric sites of CDK4. Lipinski's rule of five was used to determine the drug-likeness and the activities of the lead phytochemicals. Bioassay IC_{50} data for reported CDK4 inhibitors from the Chembl database were used to generate the 3D-QSAR model for CDK4 inhibition. The virtual screening showed catechin, kaempferol and quercetin as the lead phytochemicals. A positive correlation of 0.829 between the pIC50 and glide scores at $p<0.01$ revealed that computers can accurately predict experimental data. The ADME screening showed that naringenin, aporphine, catechin, coreximine and stepharine obey the Lipinski rules of five. The generated model was robust and thoroughly validated with a Pearson correlation R value of 0.934 and R^2 value of 0.872. The model with an adjusted R^2 value of 0.769 possesses good external validation. Aporphine, catechin, naringenin, stepharine and coreximine form important hydrogen bond interactions. These interactions are likely responsible for their inhibition of CDK4. The lead phytochemicals are drug-like compounds and potential inhibitors of CDK4.

SCAN ME

Introduction

Cancer is a disease of abnormal cell growth in which dysregulated kinase activities lead to malfunctioned cell cycle control [1]. Cyclin-dependent kinase 4 (CDK4) is a serine/threonine-protein kinase significant for regulating cell cycle progression, transcription and neuronal function of the eukaryotic cells [2]. CDK4 complex with D-type cyclins control transition through the G_1/S phase of the cell cycle [3]. The overexpression of CDK4 has been reported in various cancer types [4]. Treatment of cancer cells with cyclin-dependent kinase inhibitors prevents over-proliferation of the cancer cells [5]. Inhibition of CDK4 helps to regulate the division of cells [6]. CDK4 inhibitors induce cell cycle arrest in the G_1 phase and prevent tumor progression. While palbociclib, an inhibitor of CDK4 and CDK6, is used for the treatment of ER-positive and HER2-negative breast cancer, the toxicity associated with palbociclib, abemaciclib and flavopiridol is a major drawback in the therapeutic use of these drugs [7, 8].

Nature is known to be a source of medicinal products from time immemorial, with the large number of drugs developed from natural sources [9]. Among those, plants are known to be a rich source of diverse chemicals that could serve as the basis for rational drug design [9, 10]. A large number of phytochemicals have been reported to possess anti-cancer properties [11-14]. For example, Song et al. [15] showed vitex rotundifolia fruit limit the proliferation of human colorectal cancer cells via the downregulation of cyclin D1 and CDK4. Similarly, mangiferin extracted from *Mangifera indica* is shown to inhibit cell cycle regulator CDK4 [16]. In this study, a total of one hundred and seventy-eight (178) characterized phytochemicals from various anti-cancer plants, *Argerantum conyzoides*, *Cannabis sativa*, *Zingiber offinale*, *Annona muricata* (Graviola), *Occimum gratissimum* and *Tinospora cordifolia* were retrieved from literature and screened against the catalytic site of CDK4 to evaluate their potential as CDK4 inhibitors. The drug-likeness of the leads was determined and the 3D-QSAR model for CDK4 inhibition was equally derived.

Materials and Methods

Data collection and preparation

A total of one hundred and seventy-eight (178) characterized phytochemicals from various anti-cancer plants, *Argerantum conyzoides*, *Cannabis sativa*, *Zingiber offinale*, *Annona muricata* (Graviola), *Occimum gratissimum* and *Tinospora cordifolia* were retrieved from the literature [17-22]. The 2D structures of the phytochemicals were obtained from the NCBI PubChem database. The ligand preparation tool in Schrödinger Maestro was used to prepare the 2D structures of the phytochemicals for docking.

Protein generation and preparation

The 3-dimensional crystalized conformational structure of CDK4 was obtained from the Protein Data Bank (PDB) repository. The protein code is 2w96 with 2.3Aº. The downloaded protein was viewed with Pymol (version 2.5.0, Schrödinger, LLC, New York, NY). It has two subunits of the same amino acid sequence labeled as chain A and chain B. Schrödinger-Maestro (Schrödinger, LLC, New York, NY) was used as the graphical user interface. Protein preparation tools in Schrödinger-Maestro were used for 2w96 preparation. Missing residues were filled using the Prime tool (Prime, Schrödinger, LLC, New York, NY). Water molecules within the active site were deleted. Hydrogen atoms were added and 2w96 was optimized at pH 7.0 and minimized using the OPLS3 force field.

Glide scores, standard precision and extra-precision mode

The molecular docking of the phytochemicals into the catalytic site of CDK4 was carried using glide and the grid coordinates of the co-crystallized ligand, X= 5.57, Y= -2.67, Z=-84.04. The protein was treated as rigid, and the rotatable bonds of the phytochemicals were set free. The standard precision (SP) was used to rank the phytochemicals with respect to their glide scores. Results obtained from standard precision were subject to extra precision (XP) all in the Schrödinger-Maestro.

Validation of glide scores

The glide scores were validated by correlation coefficient analysis of the pIC_{50} values of known inhibitors of CDK4 obtained through wet experiments against their corresponding glide scores. Using the ChemBL Database, the CDK4 sequences were blasted on the Chembl (www.ebiac.uk/chembl). A total of 471 known inhibitors of CDK4 with their corresponding IC_{50} were downloaded in text format and converted to sdf format by DataWarrior version 2 [23]. The 471

compounds obtained were docked into the CDK4 catalytic site. The correlation was significant when *P* was less than 0.01.

Determination of molecular properties

According to Lipinski et al. [24], the rule of five predicts an orally active drug. Lipinski's rule of five was used to evaluate the drug-likeness and the probable biological activities of the lead phytochemicals. The Mavin Viewer software (www.chemaxon.com) was used to assess the conformity of the hit phytochemicals to the rule of five. The number of rotatable bonds and polar surface area were also determined using Mavin Viewer software [25]. Compounds with 10 or fewer rotatable bonds as well as polar surface area equal to or less than 140Å² are reported to have good oral bioavailability [25].

Quantitative structure-activity relationship

Data collection and descriptor calculation

The bioassay IC_{50} data for CDK4 was downloaded from the Chembl database in excel format and converted to sdf format (2-dimensional structures) using DataWarrior software [23]. The catenated output structures in sdf format were converted to pdb format (3-dimensional structures) with OpenBabel 2.3.1 software [26]. The chemistry development kit (CDK) was used to generate molecular descriptors for the compounds.

Data pre-treatment

The pretreatment of the bioassay IC_{50} data from the chEMBL database was carried out with V-WSP algorithm [27]. This helps to remove co-linearity among the descriptors.

Data set division: training and test sets

The data set (100 CDK4 inhibitors) was divided into the training set and test set with the aid of the Kennard Stone algorithm [28]. The data set was divided into training (70%) and test (30%) datasets.

Genetic algorithm and multiple linear regression

Genetic algorithm (GA) is a search heuristic system that behaves like the natural selection process to perform the selection of significant variables (descriptors) during QSAR model development**.** The training set was used for the model generation. The unbiased model equation was carried through multiple linear regression (MLR) and genetic algorithm.

Results and Discussion

Virtual screening

The screening of phytochemicals from the reported anti-cancer plants against the orthosteric site of CDK4 (Table S1) revealed fifteen phytochemicals with higher binding energies than the standard inhibitor of CDK4, palbociclib (Table S2). Catechin, kaemferol, and quercetin, the first three leads in this study (Table S3) have all been reported to possess anti-cancer properties [29-31].

Validation of glide score

Experimentally determined pIC_{50} of known 108 inhibitors of CDK4 obtained from cheMbl (https://www.ebi.ac.uk/chembl/) and their corresponding glide scores showed a positive correlation between pIC_{50} and glide scores at $p<0.01$ (Fig. 3; Table S3). It suffices to say that computational data can correctly predict the experimental data**.**

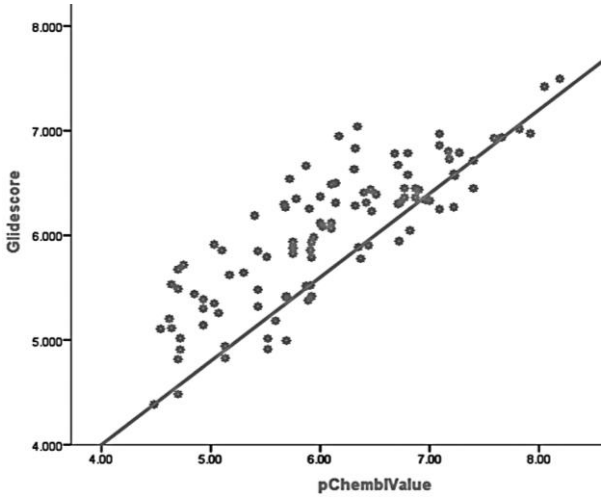

Fig. 1 Glide score versus pIC_{5b}.

Lipinski "Rule of Five" pruning

Lipinski's "rule of five" provides a platform for the selection of drug-like compounds in terms of ADME. According to Lipinski et al. [24], an orally active drug has no more than one violation of 5 H-bond donors, 10 H-bond acceptors, molecular weight (MWT) greater than 500 and the calculated Log-P (CLogP) greater than 5 (or MlogP>4.15). Also, Veber et al. [25] stated that compounds with good oral bioavailability have less than 10 rotatable bonds (NRB) and less than 140 Å polar surface area (PSA). Only naringenin, aporphine, catechin, coreximine and stepharine obeyed Lipinski's Rule

of Five (Table S4) and violated not more than the rules. The compounds, like isoboldine, isolaurine, kaempferol, quercetin, secoisolariciresinol, epicatechin, nicotinic acid and coclaurine were pruned out because those violated more than the Rule of Five.

The QSAR analysis

Quantitative structure activity (QSAR) relationship is a statistical correlation of structural and pharmacological activity quantitatively for a series of compounds. A total of 70 inhibitors of CDk4 were used as the training set. SPSS version 21 (Chicago, SPSS Inc., USA) was used in the regression analysis and model generation.

Table 1 Model summary showing the values of R, R^2, adjusted $R^2$and Durbin-Watson values.

Model	R	R^2	Adjusted R^2	Durbin-Watson
1	0.934	0.872	0.769	1.738

a. Predictors (constant), XLogP
b. Predictors
c. Dependent variable: pIC50

The adjusted R^2 was calculated using Stein's formula:

$$AdjustedR^2 = 1 - \left[\left(\frac{n-1}{n-k-1}\right)\left(\frac{n-2}{n-k-2}\right)\left(\frac{n+1}{n}\right)\right](1-R^2)$$

Where:
R^2 = measurement of the variability in the pIC_{50} accounted for by the descriptors in the model
n = number of compounds in the training set
k = number of descriptors in the model

Table 1 shows the model summary with 0.934 R^2 value of Pearson correlation. This value demonstrates an outstanding correlation between the dependent variable (pIC_{50}) and independent variables (descriptors). The R^2 value of 0.872 revealed the 3D-QSAR models could predict over 87% of the variations in the predicted pIC_{50}. The adjusted R^2 is concerned with how the model generalizes, that is, external validation of the model. The adjusted R^2 is close to the R^2 value (the difference between the R^2 value and the adjusted R^2 value is 0.103), this signifies that our model experiences just a paltry 10.3% shrinkage in predicting external pIC_{50}. The closeness of the adjusted R^2 value to the R^2 value shows that the cross validity of the model is very good. The Durbin-Watson statistics of 1.738 demonstrates that the assumption of independent error is credible, and the model is valid [32].

Model generation

The model generated from the genetic algorithm is the same as those generated in multiple linear regression (MLR), which further validated the model. Fig. 2 shows the scattered plot of the observed pIC50 values against the predicted pIC50 values of the training set using the model. The R^2 value of 0.872 depicts a strong correlation between the observed pIC50 and the predicted pIC50 and further gives credence to the robustness of the 3D-QSAR model (Table S5).

The equation of a straight line is given as:
$Y = mX+C$ eq. 1

The equation for regression is given as:

$Y = b_0+b_1x_1+b_2x_2+\ldots\ldots b_ax_b$ eq. 2

Where:
b_0 = constant
b_1 = regression coefficient
x_1 = independent variable

Therefore, the model equation is given as:

pIC_{50}=(15.024)+(5.225×XLogP)+(0.027×MW)+(0.374×TopoPSA)+(0.965×nRotB)+(5.171×nHBDon)+(1.839×nHBAcc)+(1.553×WK.unity)+(5.824×SC3)+(0.332×BCUTp11)+(2.441×MDEC3+(0.582×MDEC23)+(5.335×PetitjeanNumber)+(7.978×VP-5) eq. 3

Where:
XlogP = partition coefficient
MW = molecular weight
TopoPSA = topological Polar Surface Area
nRotB = number of rotatable bonds

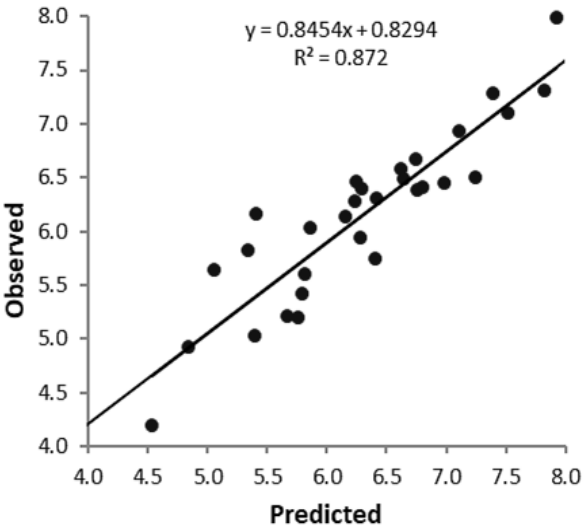

Fig. 2 Scattered plot of the observed pIC_{50} values versus the predicted pIC_{50} values of the training set.

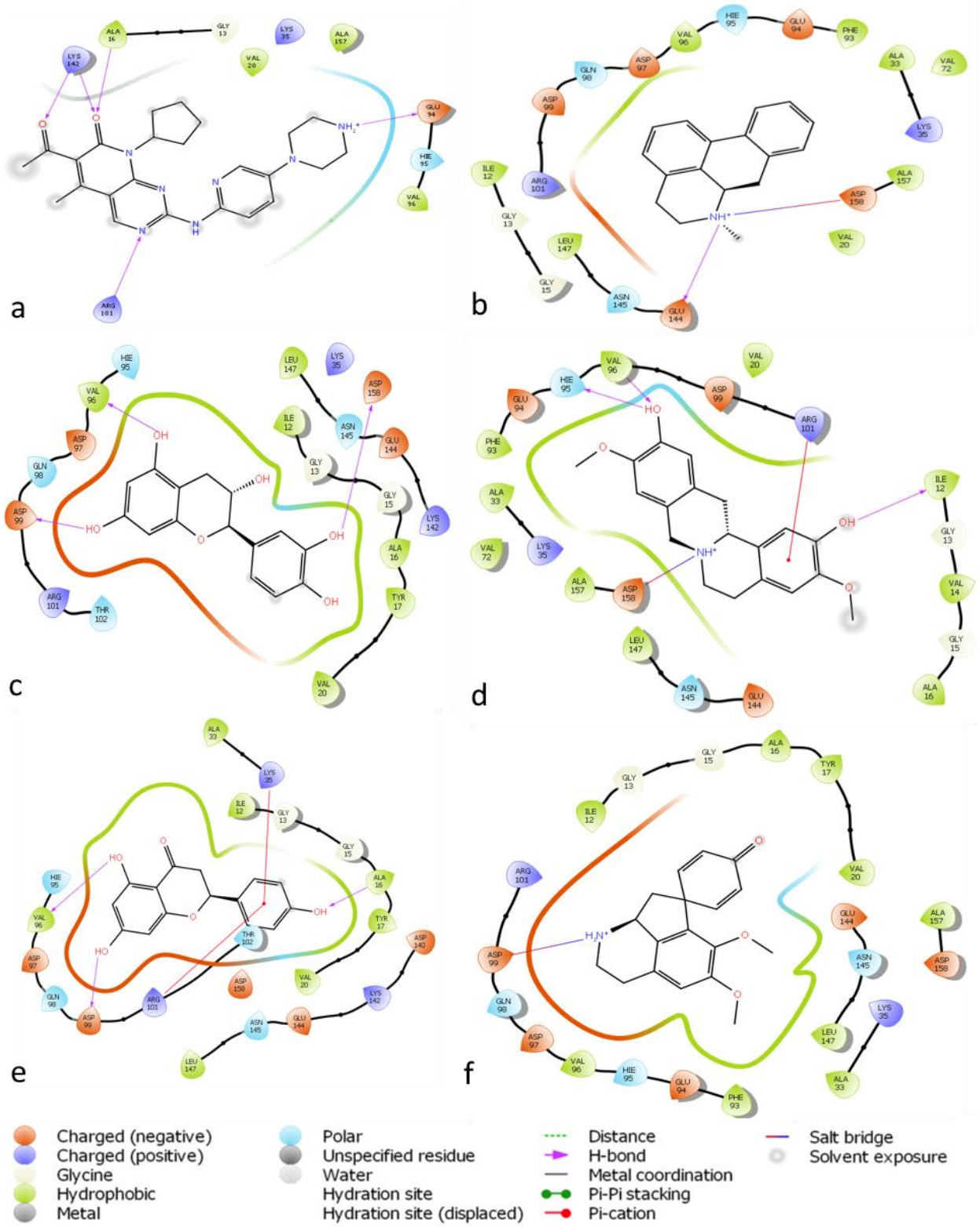

Fig. 3 Interactions of the standard drug with key residues within the catalytic sites of cyclin-dependent kinase 4 (CDK4). (**a**) Interactions of the standard drug, palbociclib with key residues within the catalytic site of CDK4; (**b**) interactions of aporphine with key residues within the catalytic site of CDK4; (**c**) interactions of catechin with key residue within the catalytic site of CDK4; (**d**) interactions of coreximine with key residue within the catalytic site of CDK4; (**e**) Interactions of naringenin with key residue within the catalytic site of CDK4; and (**f**) interactions of stepharine with key residue within the catalytic site of CDK4.

nHBDon: number of Hydrogen bond donor
nHBAcc: number of Hydrogen bond Acceptor
WK.unity: non-directional WHIM, weighted by unit weights
SC3: simple cluster, order 3
BCUTp: nhigh lowest polarizability weighted BCUTS
MDEC-34: molecular distance edge between all tertiary and quaternary carbons
MDEC-23: molecular Distance edge between all secondary and tertiary carbons Petitjean Number is the Petitjean number
Vp-5: valence path, order 5

Molecular docking interactions

It is well documented that the non-conserved residues in the ATP binding pocket of CDK4 are His95, Val96, Asp97, Arg101, Thr102 and Glu144, which are significantly different from CDK2. In CKD2, ATP binding pockets are Phe82, Leu83, His84, Lys88, Lys89 and Gln131 and in CDK6, those are Thr102 and Gln149. Arg101 alters Arg101 and Glu144 of CDK4. Arg101 and Glu144 are germane for the selective inhibition of CDK4 [33]. Molecular docking interactions shown in Fig. 3a-f, revealed all the compounds, including the standard drug are rightly situated within the ATP binding site of CDK4 and hence contribute to competitive binding inhibition of the CDK4 [34]. According to Bissantz et al. [35], Glu144, Asp158, Lys35, and Gly18 are important residues involved in hydrogen bond and Pi-cation interactions. Glu144, Val96, and/or Arg101, which are altered residues in the orthosteric site of CDK4 have been reported to be significant in the selective inhibition of CDK4 [35, 36]. The standard drug, palbociclib forms hydrogen bond interaction with Arg101 residue, known to be essential for the selective inhibition of CDK4, hence it is reported inhibitor of CDK4 [37]. Aporphine forms two hydrogen bond interactions with Glu144 and Asp158, Glu144 is an essential residue known to be significant for the selective inhibition of CDK4 [34]. Catechin form hydrogen bond interaction with significant residues, Val96 and Asp158. Val96 is known to be involved in the selective inhibition of CDK4 [33]. Coreximine form three important hydrogen bond interactions with Asp158, Arg-101 and val96. These residues are known to be responsible for selective inhibition of CDK4 [33]. Coreximine and Naringenin form hydrogen bond interactions with Arg101, Lys 35 and Val-96 (Fig. 3a-f).

Conclusions

Phytochemicals are known for their anti-cancer properties. The present study revealed novel phyto-inhibitors of CDK4. The lead compounds, catechin, aporphine, coreximine, naringenin and stepharine were perfectly situated within the ATP binding pocket of CDK4 and forms germane interactions with Glu144, Asp158, Lys35, Val96, and Arg101, which contribute to the competitive binding inhibition of CDK4. The 3DSAR mode herein is robust and thoroughly validated. The lead phytochemicals are potential inhibitors of CDK4 and are drug-like compounds.

Conflict of interest

The author declares no conflict of interest.

References

[1] Deshpande A, Peter P, Hinds PW. Cyclins and cdks in development and cancer: a perspective. Oncogene 2005; 24:2909–2915
[2] Suryadinata R, Sadowski M, Sarcevic B. Control of cell cycle progression by phosphorylation of cyclin-dependent kinase (CDK) substrates. Biosci Rep 2010; 30:243-255.
[3] Malumbres M, Barbacid M. Mammalian cyclin-dependent kinases. Trends Biochem Sci 2005; 30:630–41.
[4] An HX, Beckmann MW, Reifenberger G, Bender H, Niederacher D. Gene amplification and overexpression of CDK4 in sporadic breast carcinomas is associated with high tumor cell proliferation. Am J Pathol 1999; 154:113–8.
[5] Ortega S, Malumbres M, Barbacid M. Cyclin D-dependent kinases, INK4 inhibitors and cancer. Biochim Biophys Acta Rev Cancer 2002; 1602:73-87.
[6] Aladi EO, Hadiza RJ, Opeyemi EG, Joseph OA, Iyanuoluwa OE, Samuel AN, Damilohun MS, Idowu OO. Molecular binding signatures of Trigonella foenum-graecum compounds on cyclin-dependent kinase 4 for possible anti-cancer mechanism in breast cancer. GSC Biol Pharma Sci 2020; 11(3):014-21.
[7] Finn RS, Dering J, Conklin D, Kalous O, Cohen DJ, Desai AJ, Ginther C, Atefi M, Chen I, Fowst C, Los G. PD 0332991, a selective cyclin D kinase 4/6 inhibitor, preferentially inhibits proliferation of luminal estrogen receptor-positive human breast cancer cell lines in vitro. Breast Cancer Res 2009; 11(5):1-3.
[8] Rocca A, Farolfi A, Bravaccini S, Schirone A, Amadori D. Palbociclib (PD 0332991). targeting the cell cycle machinery in breast cancer. Expert Opin Pharmacother 2014; 15(3):407-420.
[9] Cragg GM, Newman DJ. Natural products: a continuing source of novel drug leads. Biochim Biophys Acta Gen Subj BBA-GEN 2013; 1830(6):3670-3695.

[10] Akinloye OA, Akinloye DI, Lawal MA, Shittu MT, Metibemu DS. Terpenoids from Azadirachta indica are potent inhibitors of Akt: validation of the anticancer potentials in hepatocellular carcinoma in male Wistar rats. J Food Biochem 2020; 45:e13559.

[11] Metibemu DS, Akinloye OA, Akamo AJ, Okoye JO, Ojo DA, Morifi E, et al. Carotenoid isolates of *Spondias mombin* demonstrate anticancer effects in DMBA-induced breast cancer in Wistar rats through X-linked inhibitor of apoptosis protein (XIAP) antagonism and anti-inflammation. J Food Biochem 2020; 44:e13523.

[12] Metibemu DS, Akinloye OA, Akamo AJ, Okoye JO, Ojo DA, Morifi E, et al. VEGFR-2 kinase domain inhibition as a scaffold for anti-angiogenesis: Validation of the anti-angiogenic effects of carotenoids from Spondias mombin in DMBA model of breast carcinoma in Wistar rats. Toxicol Rep 2021; 8:489–498

[13] Metibemu DS. vHTS and 3D-QSAR for the identification of novel phyto-inhibitors of farnesyltransferase: validation of ascorbic acid inhibition of farnesyltransferase in an animal model of breast cancer. Drug Res 2021; doi: 10.1055/a-1422-1885.

[14] Metibemu DS, Oyeneyin OE, Omotoyinbo DE, Adeniran OY, Metibemu AO, Oyewale MB, et al. Molecular docking and quantitative structure activity relationship for the identification of novel phyto-inhibitors of matrix metalloproteinase-2. Sci Lett 2020; 8(2):61-68.

[15] Song HM, Park GH, Park SB, Kim HS, Son HJ, Um Y, et al. Vitex rotundifolia fruit suppresses the proliferation of human colorectal cancer cells through down-regulation of cyclin D1 and CDK4 via proteasomal-dependent degradation and transcriptional inhibition. Am J Chin Med 2018; 46:191–207.

[16] Chando RK, Hussain N, Rana MI, Sayed S, Alam S, Fakir TA, et al. CDK4 as a phytochemical based anticancer drug target. bioRxiv 2019; 1:859595.

[17] Nweze NE, Obiwulu IS. Anticoccidial effects of Ageratum conyzoides. J Ethnopharmacol 2009; 122:6-9.

[18] Zhu LX, Sharma S, Stolina M, Gardner B, Roth MD, Tashkin DP, et al. Δ-9-Tetrahydrocannabinol inhibits antitumor immunity by a CB2 receptor-mediated, cytokine-dependent pathway. J Immunol 2000; 165:373-380.

[19] Habib SHM, Makpol S, Hamid NAA, Das S, Ngah W Z W, et al. Ginger extract (*Zingiber officinale*) has anti-cancer and anti-inflammatory effects on ethionine-induced hepatoma rats. Clinics 2008; 63(6):807-813.

[20] Abdul Wahab SM, Jantan I, Haque MA, Arshad L. Exploring the Leaves of *Annona muricata* L. as a Source of Potential Anti-inflammatory and Anticancer Agents. Front Pharmacol 2018; 9:661.

[21] Nangia-Makker P, Raz T, Tait L, Shekhar MP, Li H, Balan V, et al. *Ocimum gratissimum* retards breast cancer growth and progression and is a natural inhibitor of matrix metalloproteases. Cancer Biol Ther 2013;14(5):417-427.

[22] Sharma P, Dwivedee BP, Bisht D, Dash AK, Kumar D. The chemical constituents and diverse pharmacological importance of Tinospora cordifolia. Heliyon 2019; 5(9):e02437.

[23] Sander T, Freyss J, von Korff M, Rufener C. DataWarrior: An open-source program for chemistry aware data visualization and analysis. J Chem Inf Model 2015; 55:460-473.

[24] Lipinski CA, Lombardo F, Dominy BW, Feeney PJ. Experimental and computational approaches to estimate solubility and permeability in drug discovery and development settings. Adv Drug Deliv Rev 2001; 46:3-26.

[25] Veber DF, Johnson SR, Cheng HY, Smith BR, Ward KW, Kopple KD. Molecular properties that influence the oral bioavailability of drug candidates. J Med Chem 2002; 45(12):2615-2623.

[26] O'Boyle N, Banck M, James CA, Morley C, Vandermeersch T, Hutchison GR. Open Babel: an open chemical toolbox. J Cheminform 2011; 3:1–14.

[27] Ballabio D, Consonni V, Mauri A, Claeys-Bruno M, Sergent M, Todeschini R. A novel variable reduction method adapted from space-filling designs. Chemom Intell Lab Syst 2016; 136:147-154.

[28] Todd MM, Arten P, Douglas MY, Muratov EN, Golbraikh A, Zhu H, et al. Does rational selection of training and test sets improve the outcome of qsar modeling? J Chem Inf Model 2012; 52:2570-2578.

[29] Manikandan R, Beulaja, M, Arulvasu C, Sellamuthu, S, Dinesh D, Prabhu D, et al. Synergistic anticancer activity of curcumin and catechin: An in vitro study using human cancer cell lines. Microsc Res Tech 2011; 75(2):112–116.

[30] Kashyap D, Sharma A, Tuli HS, Sak K, Punia S, Mukherjee TK. Kaempferol–a dietary anticancer molecule with multiple mechanisms of action: recent trends and advancements. J Funct Foods 2017; 30:203–219.

[31] Hashemzaei M, Far AD, Yari A, Heravi RE, Tabrizian K, Taghdisi SM, et al. Anticancer and apoptosis-inducing effects of quercetin *in vitro* and *in vivo*. Oncol Rep. 2017; 38:819-28.

[32] Durbin J, Watson GS. Testing for serial correlation in least squares regression, II. Biometrika 1951; 30:159–178.

[33] Rondla R, Padma Rao LS, Ramatenki V, Haredi-Abdel-Monsef A, Potlapally SR, et al. Selective ATP competitive leads of CDK4: Discovery by 3D-QSAR pharmacophore mapping and molecular docking approach. Comput Biol Chem 2017; 71:224–229.

[34] Aubry C, Wilson AJ, Jenkins PR, Mahale S, Chaudhuri B, Maréchal JD, et al. Design, synthesis and biological activity of new CDK4-specific inhibitors, based on fascaplysin. Comput Biol Chem 2012; 4(5):787-801.

[35] Bissantz C, Kuhn B, Stahl M. A medicinal chemist's guide to molecular interactions. J Med Chem 2010; 53(14):5061-5084.

[36] Shafiq MI, Steinbrecher T, Schmid R. Fascaplysin as a specific inhibitor for CDK4: Insights from molecular modelling. PLOS One 2012; 7(8): e42612.

[37] Knudsen ES, Hutcheson J, Vail P, Witkiewicz AK. Biological specificity of CDK4/6 inhibitors: dose response relationship, *in vivo* signaling, and composite response signature. Oncotarget 2017; 8:43678-43691.